Biochem. J. (2014) **459**, 355–368 (Printed in Great Britain) doi:10.1042/BJ20130847

online data

Differential functions of calpain 1 during epithelial cell death and adipocyte differentiation in mammary gland involution

Teresa ARNANDIS*, Ivan FERRER-VICENS*, Luis TORRES*, Concha GARCÍA*, Elena R. GARCIA-TREVIJANO*, Rosa ZARAGOZA* and Juan R. VIÑA*[1]

*Departamento de Bioquímica y Biología Molecular, Fundación Investigación Hospital Clínico-INCLIVA, Facultad de Medicina, Universidad de Valencia, Valencia 46010, Spain

Calpains become activated in the mammary gland early during weaning, cleaving several proteins located mainly in the cell membrane, but also in other organelles such as lysosomes, mitochondria and nuclei. By immunofluorescence and Western blot analysis, we have demonstrated the nuclear translocation of calpain-1 and calpain-2, together with the cleavage of several cytoplasmic nucleoporins in epithelial cells of the lobulo-alveolar compartment. *In vivo* and *in vitro* calpain inhibition prevented this nucleoporin degradation. In addition, calpain-1 was also present in the nucleus of non-epithelial mammary tissue cells, concomitant with adipocyte re-differentiation. Calpain-1 was internalized within nuclei and found to be present in the nuclear chromatin-enriched fraction, associated with histone H3. Furthermore, we have demonstrated, both *in vivo* and *in vitro*, the cleavage of the N-terminal residue of histone H3 by calpain-1. Calpain-1 co-localized with both H3K4me3 (histone H3 trimethylated at Lys^4) and H3K27me3 (histone H3 trimethylated at Lys^{27}) at the nuclear periphery, a bivalent epigenetic signal essential for cell differentiation. Using ChIP assays we could confirm the presence of calpain-1 in the promoters of key genes expressed in adipose tissue, such as *Cebpa* (CCAAT/enhancer-binding protein α) and *Lep* (leptin). The results of the present study highlight a dual role for calpain-1 in the weaned gland after the pregnancy/lactation cycle, controlling programmed cell death and participating in the epigenetic programme during adipocyte differentiation.

Key words: adipocyte differentiation, calpain, cell death, histone H3 cleavage, nucleoporin, nuclear permeability.

INTRODUCTION

The weaning process after the pregnancy/lactation cycle, also known as involution, has two phases. The first is reversible, and is characterized by the disappearance of the physiological adaptations and programmed cell death in the epithelial cells of the lobulo-alveolar compartment in the mammary gland. The second phase is irreversible and includes a proteolytic degradation of the basement membrane, remodelling of the mammary gland and epithelial cell replacement due to adipocyte differentiation and proliferation [1].

Over the last years, several signalling pathways have been described to regulate the whole process of involution [2–4]. Among them, the STAT (signal transducer and activator of transcription) signalling pathways regulate epithelial cell death [5,6] and the RARα (retinoic acid receptor α) pathway controls MMP-9 (matrix metalloproteinase-9) expression during involution, thus regulating matrix remodelling [7]. Recently, NF-κB (nuclear factor κB) was revealed as a major factor regulating mouse mammary gland involution. We have identified 268 NF-κB target genes by ChIP-chip in mouse mammary glands after 48 h of weaning [8]. Among them, *Capn1* (calpain-1) and *Capn2* were identified. The transactivating form of NF-κB^{p65}/p300 was found to bind the *Capn1* and *Capn2* promoters with the subsequent induction of gene expression after 48 h of weaning [9].

Calpains are a family of multidomain intracellular enzymes that share a calcium-dependent cysteine protease core [10]. The most abundant members are CAPN1 and CAPN2. They are heterodimers, consisting of a small regulatory subunit (30 kDa) and a large catalytic subunit (80 kDa). These isoforms differ in the calcium concentration required for their activation *in vitro* [11], and coexist with calpastatin, their endogenous specific inhibitor [12]. Calpains have been demonstrated to mediate epithelial cell death during mammary gland involution; however, since calpains can cleave a variety of sequences on non-related proteins [10] the different pathways in which these proteases are involved remain elusive. We have reported previously a role for these enzymes in mitochondrial- and lysosomal-mediated cell death [9]. The aim of the present study was to unveil other possible roles for calpains in mammary gland involution.

It has been reported previously that in different cell types, upon transient elevation of intracellular calcium, calpains can undergo specific subcellular relocation from the cytosol to the nucleus, where they can proteolyse transcription factors and nuclear proteins [13,14]. Indeed, cross-talk between the nucleus and other intracellular compartments is tightly co-ordinated. NPCs (nuclear pore complexes), with multiple copies of roughly 30 different NUPs (nucleoporins), comprise aqueous channels that penetrate the nuclear envelope connecting the nucleus and the cytoplasm [15]. Calpains could translocate to the nuclear membrane during mammary gland involution, playing a role in the orchestration of cell death through the modulation of NPCs.

Moreover, calpains are required for differentiation of mesenchymal stem cells of different lineages, such as myoblastic, osteoblastic, chondrocytic and adipocytic [16], and regulating the differentiation of 3T3-L1 pre-adipocytes into adipocytes. Calpain control of adipogenesis involves transcriptional activation of C/EBPα (CCAAT/enhancer-binding protein α), which functions as a pleiotropic transcriptional activator of numerous adipocyte genes, such as *Lep* (leptin), *Adipoq* (adiponectin) or *Pparg*

Abbreviations: ALLN, *N*-acetyl-L-leucyl-L-leucylnorleucinal; CAPN, calpain; C/EBPα, CCAAT/enhancer-binding protein α; COXIV, cytochrome *c* oxidase IV; GADPH, glyceraldehyde-3-phosphate dehydrogenase; H3K4me3, histone H3 trimethylated at Lys^4; H3K27me3, histone H3 trimethylated at Lys^{27}; IPO8, importin 8; Lep, leptin; LAMP2, lysosomal-associated membrane protein 2; MBP, myelin basic protein; NF-κB, nuclear factor κB; NPC, nuclear pore complex; NUP, nucleoporin; qPCR, quantitative real-time PCR; TGN38, *trans*-Golgi network protein 2.

[1] To whom correspondence should be addressed (email Juan.R.Vina@uv.es).

(peroxisome-proliferator-activated receptor γ); the latter is considered as the master regulator of adipogenesis together with C/EBPα [17,18]. In the present study, we identify the nuclear compartment as another target of calpain-mediated cell death, in addition to the well-described lysosomal and mitochondrial pathways. More importantly, we show a differential role of CAPN1 in the nuclei of mammary gland cells after weaning, although CAPN1, upon nuclear membrane translocation and NUP degradation, participates in epithelial cell death, it also seems to have an important role in adipocyte differentiation and fat pad repopulation. Indeed, the results of the present study suggest that CAPN1 regulates histone H3 cleavage. Although further studies should be undertaken, we propose a challenging role for this modification as a possible change in the 'epigenetic signature' of adipocytes upon differentiation. Taken together, the results of the present study reveal important and novel nuclear functions of this family of calcium-dependent proteases in mammary gland remodelling.

EXPERIMENTAL

Animals and tissue extraction

C57BL/6 mice were obtained from Taconic. Virgin female mice (10 weeks old) were mated and males were subsequently removed at mid-gestation. Following parturition, litters were maintained with at least seven pups. Then, at the peak of lactation (days 9–11), mice were divided into different groups: control lactating mice and weaned mice whose pups were removed 10 days after delivery to initiate involution. The weaning took place for 6, 24, 48 and 72 h before death. Mice were intraperitoneally given a single dose of sodium pentobarbital (60 mg/kg of body mass) freshly dissolved in 0.9 % NaCl (Braun Medical). Then, the inguinal mammary glands were removed and quickly freeze-clamped in liquid nitrogen or fixed in formaldehyde for histological studies. All the animals were given food and water *ad libitum* and housed in a controlled environment (12 h light/12 h dark cycle). Experimental protocols were approved by the Research Committee of the School of Medicine (University of Valencia, Valencia, Spain). The mice were cared for and handled in conformance with National Institutes of Health guidelines and the *Guiding Principles for Research Involving Animals and Humans* approved by the Council of the American Physiological Society.

Materials

Primary antibodies against GADPH (glyceraldehyde-3-phosphate dehydrogenase; ab8245), calnexin (ab22595), COXIV (cytochrome *c* oxidase; ab33985), LAMP2 (lysosomal-associated membrane protein 2; ab13524), Nup107 (ab73290), Nup153 (ab93310), Capn1 (C-terminal domain; ab39170), Capn1 (C-terminal domain) for immunoprecipitation assays (ab39171), Capn1 (N-terminal domain; ab28257), Capn2 (N-terminal domain; ab39165) and aldolase (ab71433) were purchased from Abcam. Other antibodies used were: anti-TGN38 (*trans*-Golgi network protein 2; catalogue number sc-33784; Santa Cruz Biotechnology), anti-α-tubulin (catalogue number sc-5286; Santa Cruz Biotechnology), Mab414 (catalogue number MMS-120 R; Covance), anti-Nup98 (catalogue number Mab6758; Abnova), anti-Capn2 (C-terminal domain) for immunofluorescence (catalogue number 2539; Cell Signaling Technology), anti-perilipin (catalogue number 651156; Progen Biotechnik), anti-(histone H3) (C-terminal domain; catalogue number 07-690; Millipore) and anti-(histone H3) (N-terminal domain; catalogue number 39763; Active Motif). Histone H3 markers were studied using anti-H3K4me3 (histone H3 trimethylated at Lys^4; ab12209) and -H3K27me3 (histone H3 trimethylated at Lys^{27}; ab6002), both from Abcam. Recombinant proteins and calpain inhibitors were all from Calbiochem, recombinant Capn2 (catalogue number 208718), calpain inhibitor VI (catalogue number 208745), calpeptin (catalogue number 03-34-0051), and ALLN (*N*-acetyl-L-leucyl-L-leucylnorleucinal; catalogue number 208719), except recombinant CAPN1 (catalogue number C-6108) and recombinant histone H3 (catalogue number 14-494) that were obtained from Sigma and Millipore respectively.

Calpeptin administration *in vivo*

Calpain inhibitor studies were carried out in 10-day lactating mice, in which pups were removed before the first administration. Calpeptin was dissolved in DMSO (20 mg/ml) and further diluted in physiological saline (10 mg/ml). A 40 mg/kg of body mass dose was administered by intraperitoneal injection every 12 h for 3 days. A second group of control mice received vehicle alone. After 3 days, inguinal mammary glands were removed and freeze-clamped in liquid nitrogen until further use.

Depletion of *Capn1* in mouse mammary gland

Lactating mice at the peak of lactation were forced weaned and treated with *Capn1* siRNAs from Sigma (Mission® esiRNA; catalogue number EMU057001) for 3 days. siRNA (5 μg/24 h for 3 days) mixed with L-PEI (in vivo-jetPEI™, PolyPlus-Transfection) were injected with a needle locally into the inguinal mammary glands following the manufacturer's instructions. A surgical incision of the skin was not performed; however, successful transfection of *Capn1* siRNAs was confirmed by Western blotting analysis of mammary tissue homogenates.

Immunofluorescence analysis

For immunohistochemistry, 5-μm sections from control and involuting mammary glands were treated as described previously [9]. Sections were incubated overnight at 4 °C with one of the following primary antibodies: anti-Capn1, anti-Capn2, Mab414, anti-(histone H3) N-terminal domain, anti-perilipin, anti-H3K4me3 or anti-H3K27me3. Nuclei were counterstained with Hoechst 33342 (Invitrogen) and images were acquired on a Leica TCS-SP 2 confocal microscope. Quantification of Capn1- and H3K4me3- or H3K27me3-positive cells ($n = 3$ for each co-immunofluorescence staining) in mammary stroma of 48-h involuting mice was performed. The fluorescence pattern of Capn1 and of histone modifications were measured at the optimal focal plane (2D) for each nucleus using the image processing software ImageJ (http://rsbweb.nih.gov/ij/).

Total protein extraction and immunoblotting

Total protein was extracted from snap-frozen mammary glands (0.1 g) by homogenization in a buffer containing detergents and protease inhibitors as described previously [6]. Equal amounts of protein (15 μg) were separated by SDS/PAGE (8–13.5 % gel) and transferred on to nitrocellulose membranes (Protran®; Whatman). After the addition of the corresponding primary antibody, immunocomplexes were revealed with an HRP (horseradish peroxidase)-conjugated secondary antibody (Dako), and a subsequent peroxidase ECL reaction (ECL Detection Kit; GE Healthcare). The intensity of the bands was measured

by densitometry using ImageJ. Equal loading was confirmed by reprobing the blot against α-tubulin and by Ponceau Red staining.

Subnuclear fractionation: isolation of nuclei and chromatin-enriched extracts

For nuclei isolation the Nuclear Extract kit (Active Motif) was used according to the manufacturer's instructions, followed by a subnuclear fractionation. Briefly, inguinal mammary glands were minced and homogenized in a Dounce glass homogenizer with hypotonic buffer and centrifuged at 850 ***g*** for 10 min to collect the cells. The cells were lysed by 15 min incubation in hypotonic buffer supplemented with detergents. After this incubation, nuclei were collected by centrifugation (14 000 ***g*** for 1 min at 4 °C) and supernatant recovered as cytosolic fraction. This pellet, including mainly intact nuclei, was lysed in a rocking platform for 30 min with gentle agitation. Soluble (soluble nuclear extracts) and insoluble fractions (chromatin-enriched) were then separated by centrifugation (14 000 ***g*** for 10 min at 4 °C) as the supernatant and pellet respectively. The chromatin-enriched pellets were subsequently washed with a buffer containing 3 mM EDTA, 0.2 mM EGTA, 1 mM DTT and protease inhibitor cocktail, sonicated and finally resuspended in SDS/Laemmli buffer as described previously [19].

Purification of adipocytes within the mammary tissue

To obtain the adipocyte fraction a modified version of an existing protocol was used [20]. Mammary gland tissue was minced into small pieces (3–4 mm^2) and placed into sterile plastic tubes with Krebs–Ringer buffer containing 25 mM $NaHCO_3$, 11 mM glucose, 25 mM Hepes (pH 7.4) and 1.5 mg/ml collagenase A (Roche). The ratio between adipose tissue and incubation solution was 1:4 (w/v). The tissue suspension was incubated at 37 °C with gentle shaking for 60 min. Once digestion was completed, samples were passed through a sterile 250-μm nylon mesh. The filtrate was then centrifuged at 200 ***g*** for 10 min; the floating cells were considered as the adipocyte-enriched fraction and the lower phase the stromal vascular cells including pre-adipocytes. The adipocytes were washed twice with the buffer mentioned above and centrifuged as above. After washing, the adipocyte fraction was subjected to sonication and SDS/Laemmli sample buffer was added for immunoblotting. To obtain mRNA from adipocyte extracts, the RNeasy Lipid Tissue kit from Qiagen was used.

In vitro calpain assay in nuclear extracts

Analysis of nuclear permeabilization was performed using soluble nuclear extracts, isolated as mentioned above. These were incubated for 15 min at 37 °C with different units of recombinant CAPN1 and CAPN2 in the presence of calcium (0.5 and 5 mM respectively). After the incubation, samples were dissolved in SDS/Laemmli buffer and nucleoporin degradation was analysed by Western blotting. Finally, to confirm calpain-mediated cleavage of nucleoporins, several inhibitors were used. Nuclear extracts were incubated as described above, but supplemented with different concentrations of either calpeptin (15 and 50 μM), calpain inhibitor VI (50 and 100 μM) or ALLN (50 and 100 μM).

In vitro analysis of histone H3 proteolysis was also performed using soluble nuclear extracts. Nuclear extracts from lactating (0 h) and weaned mice (48 and 72 h) were incubated for 15 min at 37 °C with recombinant histone H3. After the incubation, the reaction was stopped by dissolving the samples in SDS/Laemmli buffer and finally N-terminal fragmentation of histone H3 was analysed by Western blotting. In some cases, specific calpain inhibitors were used. Conversely, lactating nuclear extracts, where histone H3 was intact, were incubated with recombinant CAPN1 in the presence of calcium and calpain inhibitors (15 and 50 μM calpeptin) were also added to demonstrate calpain specificity.

Identification of cleaved histone H3

Both recombinant histone H3 (2.5 μg) and recombinant CAPN1 (2 units) were incubated for 15 min at 37 °C in a buffer containing 50 mM Tris/HCl (pH 7.5) to allow for calpain-mediated H3 cleavage. The incubation mixture was then subjected to SDS/PAGE (13.5 % gel) and stained with Coomassie Blue. The cleaved band was excised from the gel and MS/MS analysis was performed, as described previously [9], by the Proteomics and Bioinformatics Unit, Centre for Applied Medical Research (CIMA) at the University of Navarra (Pamplona, Spain).

Besides this MS identification of histone H3, in order to predict the most likely cleavage site a molecular mass comparison analysis was performed using ImageQuant TL software [21]. This analysis revealed one cleavage site on histone H3, between Lys^9 and Ser^{10}. This cleavage site obtained *in vitro* with recombinant proteins is the same as the one observed *in vivo* during mammary gland involution.

Immunoprecipitation

Nuclear proteins (300 μg) isolated from control and 48 h-weaned mammary glands were precleared with Protein A/G–Sepharose 50:50 (v/v) (GE Healthcare) for 1 h at 4 °C. Supernatants were immunoprecipitated overnight with 2 μg of anti-Capn1 (C-terminal domain) and 0.3 μg of Mab414 or normal serum IgG antibodies (as an unrelated antibody) at 4 °C on a rotating device. The immunocomplexes were pulled down by adding 50 μl of Protein A/G–Sepharose 50:50 (v/v). The supernatants were discarded and each pellet was thoroughly washed in PBS. The immunocomplexes were boiled in sample buffer and then subjected to SDS/PAGE (8 % gel for CAPN and 13.5 % gel for histone H3) as described previously. One percent of the total protein extracts used for immunoprecipitation was loaded as the input. Representative results of three separate experiments are shown.

ChIP assays and PCR

Chromatin from mammary tissue was fixed and immunoprecipitated as described previously [8], with anti-Capn1 (C-terminal domain) antibody. After DNA purification, the input, immunoprecipitated and unrelated antibody fractions were analysed by PCR with specific primers against the promoter region of *Cebpa* (− 315 bp) (forward, 5′-TGACTTAGAGGCTTAAAGGA-3′ and reverse, 5′-CGGGGACCGCTTTTATAGAG-3′), *Lep* (− 323 bp) (forward, 5′-GCCTTCTGTAGCCTCTTGCT-3′ and reverse, 5′-GCTCCATGCCCTGCCTGC-3′) and *Mbp* (myelin basic protein; − 372 bp) (forward, 5′- TTGTGTCCAAAGAAGCAGCG-3′ and reverse, 5′- AGAGGTCTAAATGGCATCGC-3′). PCR fragments were size-fractionated using 2 % agarose gel electrophoresis and stained with Ethidium Bromide.

For quantitative PCR, the ChIP products were amplified by quantitative PCR using the Fast SYBR Green Master mix (Applied Biosystems) following the manufacturer's instructions. The results are expressed as the fold enrichment for *Capn1* over the *Cebpa* and *Lep* promoters using the formula $2^{C_T\text{Input}-C_T\text{IP}}$.

qPCR (quantitative real-time PCR) analysis

Total RNA from mammary tissue was extracted by TRIzol® (Invitrogen) followed by additional column purification (RNeasy; Qiagen). RNA quantity and purity were determined using the NanoDrop ND-2000 (NanoDrop Technologies), and RNA integrity was assessed by determination of the RNA 28S/18S ratio using RNA 6000 Nano Labchips in an Agilent 2100 Bioanalyzer (Agilent Technologies).

RNA (500 ng) was reverse-transcribed into cDNA at 37 °C for 60 min and 95 °C for 5 min using a high-capacity RNA-to-cDNA kit (Applied Biosystems). The cDNA products were amplified by quantitative PCR using the GeneAmp Fast PCR Master mix (Applied Biosystems). All reactions were carried out in triplicate. qPCR was performed using the 7900HT Fast Real-Time PCR system. Pre-developed Taqman primers specific for *Capn1*, *Cebpa*, *Lep* and *Ipo8* (importin 8) were purchased from Applied Biosystems. Results were normalized according to *Ipo8* quantification, an appropriate housekeeping gene used in adipose tissues [22], in the same sample reaction. The threshold cycle (C_T) was determined and then the relative gene expression was expressed as: relative amount $= 2^{-\Delta(\Delta C_T)}$, where $\Delta C_T = C_T$ (target) $- C_T$ (*IPO8*) and $\Delta(\Delta C_T) = \Delta C_T$ (weaned) $- \Delta C_T$ (control).

Statistics

Results are presented as means $\pm$ S.E.M. and were analysed using one-way ANOVA. Significant differences were determined using a Tukey–Kramer test. Differences were considered significant at $P < 0.05$, and in the Figures different superscript letters indicate significant differences. The letter 'a' always represents the lowest value within the group. Independent experiments were conducted with a minimum of three replicates per condition to allow for statistical comparison.

RESULTS

Active calpains translocate to the nucleus during mammary gland involution

The calpain system has been reported previously to have a role in the nucleus of different cell types [14,23,24]. Since we have already demonstrated calpain translocation to the mitochondria and lysosomes during weaning, we investigated the possible role of these proteases in the nuclear compartment. Using purified nuclear fractions, CAPN1 translocation into the nucleus was observed at 72 h post-weaning (Figure 1A) using Western blotting. Moreover, CAPN1 and CAPN2 were active at this time point both in the cytosolic and nuclear fractions. This fact was demonstrated by the cleavage of the N-terminal domain, which is autoproteolysed upon calcium activation. The purity of nuclear fractions was assessed by Western blotting using antibodies against different organelle markers (Figure 1B). Tissue sections from 72 h post-weaning mammary glands were immunostained for CAPN1 or CAPN2. The immunofluorescence signal was observed surrounding the periphery of nuclei in scattered epithelial cells for both calpains (Figure 1C, arrowheads). To confirm that calpains are indeed interacting with the nuclear membrane, an immunoprecipitation assay was performed. Tissue extracts from control lactating (0 h) or 72 h post-weaned mice were incubated with the Mab414 antibody, which recognizes the core of several peripheral NUPs. A Western blot analysis using antibodies against CAPN1 or CAPN2 showed that both proteases

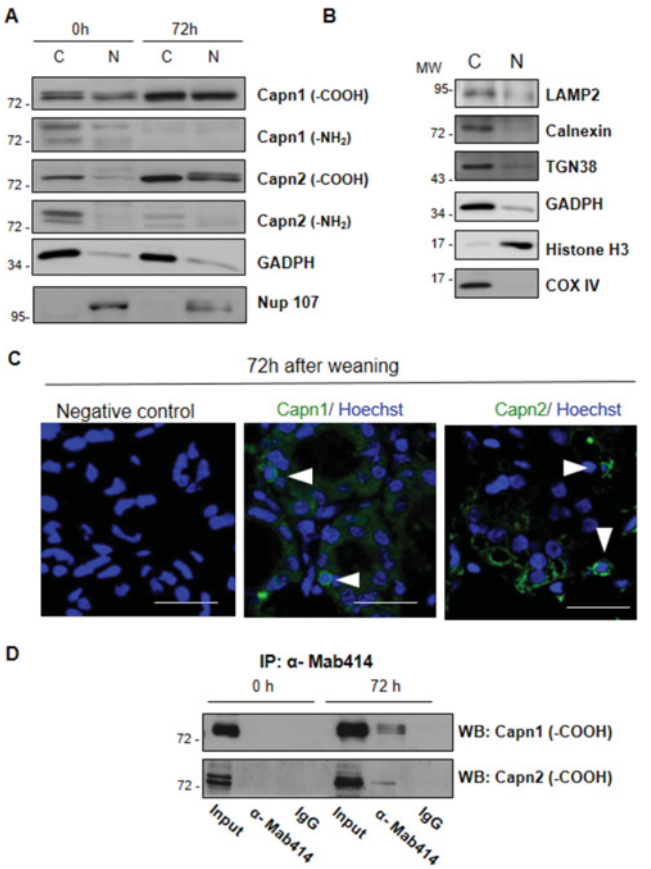

Figure 1 Calpains are present and active within nuclear fractions during mammary gland involution

(**A**) Western blot analysis of CAPN1 and CAPN2 in nuclear (N) and cytosolic (C) extracts at day 10 of lactation (0 h) and 72 h of involution after pup removal. Anti-calpain antibodies against C-terminus (-COOH) and N-terminus (-NH_2) domains were used. Cytosolic (GADPH) and nuclear (NUP107) markers were used to confirm the purity of the fractions. (**B**) Immunoblots of cytoplasmic and nuclear extracts were performed in lactating mice using antibodies against specific organelle markers: LAMP2 (lysosomal marker), calnexin (endoplasmic reticulum marker), TGN38 (Golgi apparatus), GADPH (cytosol), histone H3 (nuclei) and COXIV (mitochondrial marker). In both (**A**) and (**B**), at least three separate mice were used. (**C**) Representative immunohistochemical analysis of CAPN1 and CAPN2 in tissue sections from mammary gland after 72 h of weaning ($n = 5$). Samples were fixed and stained for CAPN1 (green), CAPN2 (green) or Hoechst 33342 (blue). Dilution buffer or secondary antibody was used to block autofluorescence or non-specific binding. Scale bars, 37.5 μm. Arrowheads point to positive calpain-staining surrounding nuclear periphery. (**D**) Co-immunoprecipitation of the Mab414 antibody and CAPN1 or CAPN2 in whole extracts from control (0 h) and 72 h-weaned glands. Samples were immunoprecipitated (IP) with the Mab414 antibody or unrelated normal serum IgG. The immunoprecipitated NUPs were analysed by Western blotting (WB) with anti-CAPN1 or -CAPN2 antibodies ($n = 3$).

were pulled down in immunoprecipitated samples from 72 h post-weaned mice (Figure 1D).

Calpain nuclear translocation was further assessed by Western blotting of the nuclear extracts from mammary tissue obtained at different times after litter removal. As demonstrated in Figure 2(A), both proteases increased their nuclear presence from 48 h of involution onwards. The quantification and statistical analysis of the translocation is shown in Figure 2(B). Regarding the possible role of calpains in the nuclear compartment, we show that several peripheral NUPs were degraded during involution and this proteolysis could be calpain-mediated. The breakdown of NUPs seems to be limited to the peripheral NPC, since NUP107, which is part of the scaffold of the NPC, was not affected (Figure 2A). Interactions of CAPN1 and CAPN2 with NUPs at

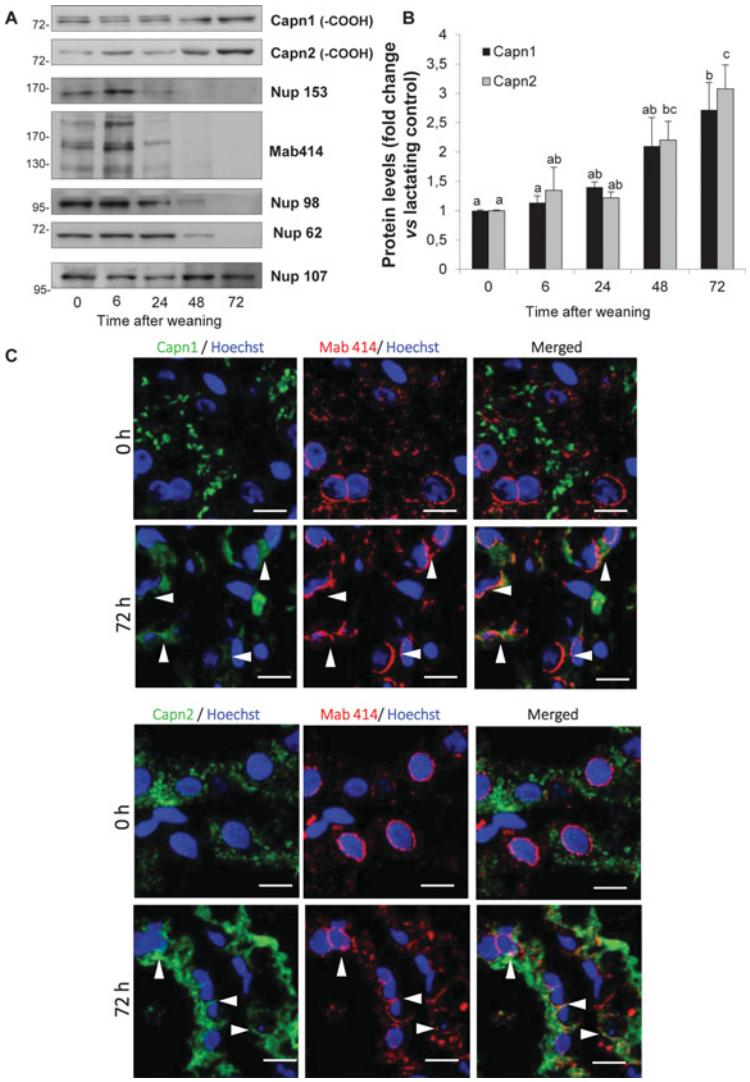

Figure 2 Calpains mediate peripheral NUP degradation

(**A**) Representative Western blot of both CAPN1 and CAPN2 in mammary gland nuclear extracts at day 10 of lactation (0 h), and 6, 24, 48 and 72 h after pup removal. Specific antibodies against Nup153, Nup98, Nup62, Nup107 and Anti-Mab414 (pan-NUP) were used. At least three different mice per developmental stage were analysed. (**B**) Quantification of CAPN1 and CAPN2 levels during involution compared with the control lactating levels. Results are means $\pm$ S.E.M. ($n = 3$). ANOVA was performed for the statistical analysis and different letters indicate significant differences ($P < 0.05$); 'a' always represents the lowest value within the group. (**C**) Representative immunofluorescence staining for NUPs and calpains in the mammary gland. Mammary tissue sections from control lactating (0 h) or 72 h involution were fixed and immunostained with the Mab414 antibody (red) and anti-CAPN1 or -CAPN2 antibodies (green). Despite the diffuse pattern of the calpain signal observed at 72 h after weaning, the arrowheads show co-localization of both calpains with Mab414. No co-localization was observed in the lactating controls. Nuclei were visualized by Hoechst 33342 (blue). Scale bars, 7 μm.

72 h of involution are shown in Figure 1(D). In order to compare involuting tissue with the lactating controls, co-immunostaining of both calpains with the Mab-414 antibody was performed. In Figure 2(C), co-localization of calpains with nucleoporins in the periphery of nuclear membranes is shown (arrowheads), corroborating the results obtained from Western blotting of the nuclear fractions (Figure 2A). However, the CAPN1 and CAPN2 fluorescent signals showed a preferential cytoplasmic localization, in agreement with their role degrading targets from mitochondrial, lysosomal and plasma membranes [9,11,13].

In vivo and *in vitro* inhibition of calpains prevents NUP cleavage

To study calpain-mediated degradation of NUPs, several approaches were carried out. *In vivo* inhibition of CAPN1, either by siRNA against *Capn1* or by the pharmacological inhibitor calpeptin, completely blocked peripheral NUP degradation at 72 h of involution, as demonstrated by Western blotting with the Mab414 and anti-Nup62 antibodies (Figures 3A and 3B respectively). When siRNA was used, CAPN1 levels were significantly reduced, whereas CAPN2 was not affected (Figure 3A, upper panels). In calpeptin-treated mice the levels of total calpains were not affected; however, the activation of CAPN1 was prevented since the N-terminal domain of this enzyme was not cleaved (Figure 3B, top line).

A cell-free assay where isolated nuclear extracts from control lactating glands were incubated with recombinant calpains further confirmed calpain-mediated cleavage of NUPs (Figure 3C). These *in vitro* studies clearly showed that peripheral NUPs disappeared when nuclear fractions were incubated with increasing concentrations of CAPN1 or CAPN2 in the presence

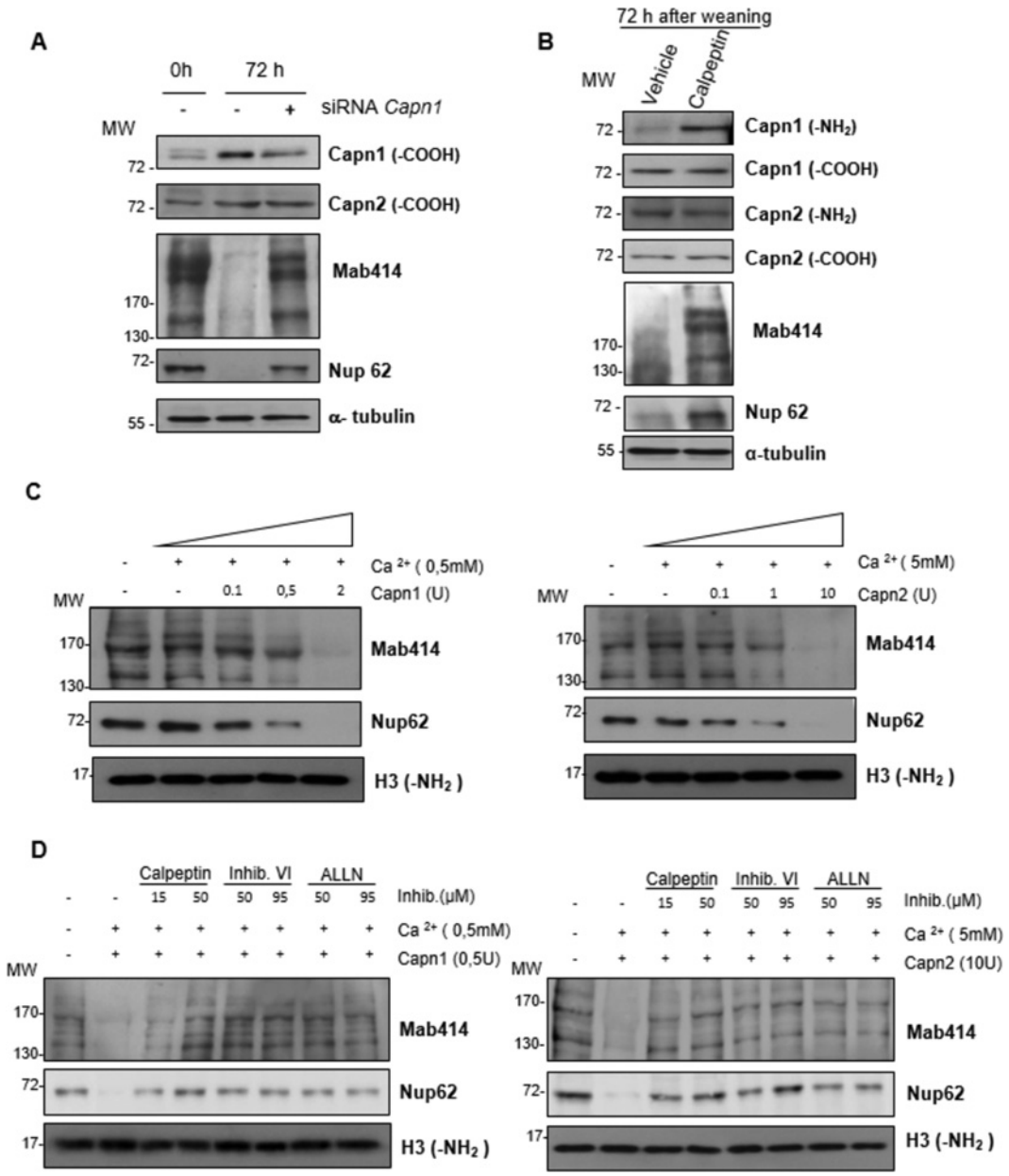

Figure 3 Inhibition of calpains prevents NUP cleavage both *in vivo* and *in vitro*

(**A**) Representative Western blot analysis of CAPN1 and CAPN2 in lactating control mice (0 h), 72 h-weaned mice and 72 h-weaned mice where CAPN1 was knocked down by specific siRNA treatment (siRNA *Capn1*). (**B**) Western blot analysis showing levels of CAPN1 and CAPN2 (using antibodies against the N- and C-terminal domains), Mab414 antibody and Nup62 in extracts from calpeptin-treated or untreated (vehicle) mammary glands at 72 h after litter removal. α-Tubulin was used as loading control. (**C**) and (**D**) Western blot analysis of Nup62 and FGFX repeat-containing NUPs (Mab414) in nuclear-enriched fractions from control lactating mammary glands incubated with increasing concentrations of either recombinant CAPN1 (left-hand panels) or CAPN2 (right-hand panels) in the presence of calcium (**C**) and a battery of inhibitors: calpeptin, calpain inhibitor VI and ALLN (**D**). Anti-(histone H3) (N-terminal domain) (-NH_2) was used as a loading control. Experiments were carried out with three different mice per experimental condition. MW, molecular mass.

of calcium. In the absence of CAPN and/or calcium no NUP cleavage was observed. Furthermore, when several calpain inhibitors were added to these nuclear extracts in the presence of recombinant calpains NUP degradation was also blocked (Figure 3D), demonstrating the direct involvement of calpains in nuclear membrane destabilization during weaning.

NUP cleavage would alter NPCs with the subsequent impairment of nuclear transport selectivity [25,26]. Indeed, the intranuclear accumulation of cytoplasmic proteins, such as tubulin and aldolase, demonstrated an increased nuclear permeability 72 h after removal of the pups (Figure 4A). A consequence of this progressive alteration would be the transfer of cytoplasmic proteins into the nuclei, as shown in Figure 4(B), where α-tubulin translocated from the cytosolic into the nuclear fraction as involution progressed.

CAPN1 is present in non-epithelial mammary tissue cells and has a role in adipocyte subpopulation

Immunofluorescence of CAPN1 in mammary gland indicated that this protease seemed to be present not only surrounding the nuclei

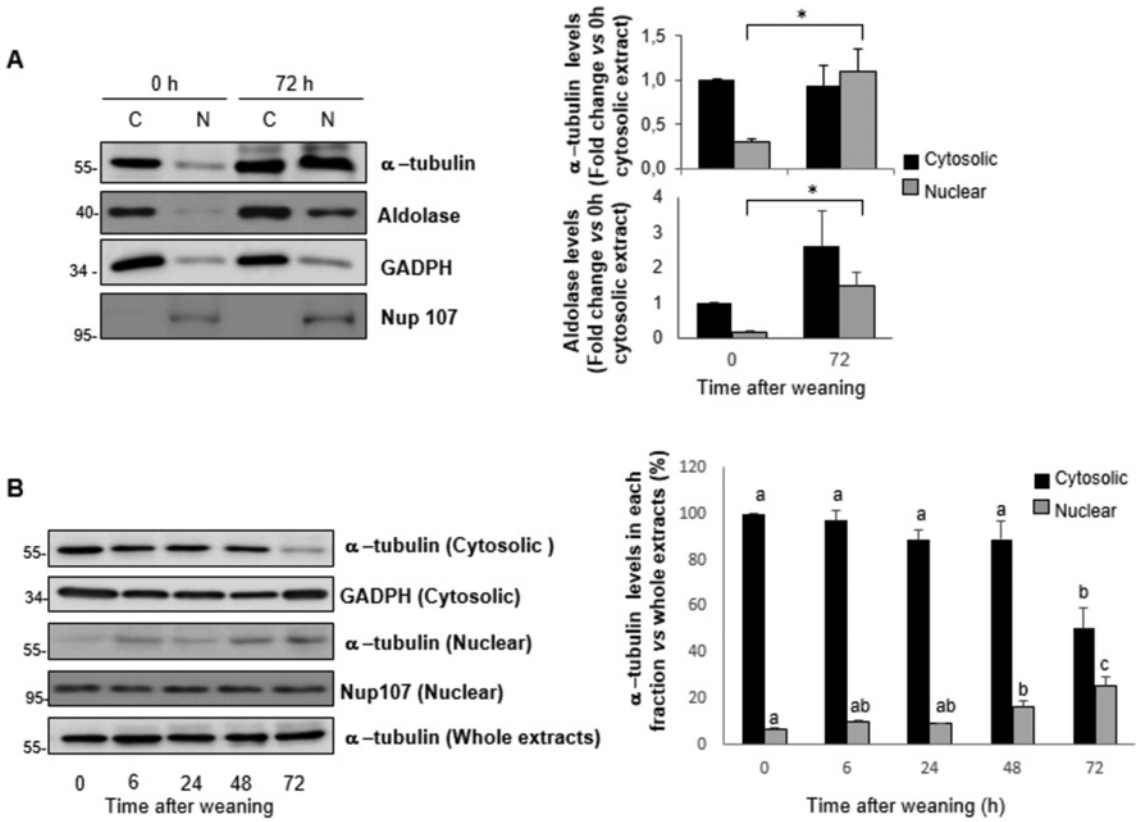

Figure 4 Increased nuclear permeability in epithelial cells during involution

(**A**) Western blot analysis of α-tubulin and aldolase in nuclear and cytosolic extracts from lactating control (0 h) and 72 h of involution. Anti-GADPH and anti-Nup107 antibodies were used as cytosolic (C) and nuclear (N) markers respectively. The intensities of α-tubulin and aldolase bands were quantified by densitometry and plotted (right-hand panel) against the cytosolic levels of control mice. Results are expressed in arbitrary units are means $\pm$ S.E.M. ($n = 4$). Student's t test was performed for the statistical analysis, $^*P < 0.05$, 0 h compared with 72 h in the nuclear extracts. (**B**) Western blot analysis of α-tubulin in cytosolic, nuclear and whole protein extracts from lactating control (0 h) and 6, 24, 48 and 72 h of involution. Cytosolic GADPH and nuclear Nup107 markers were also assessed. α-tubulin quantification in the nuclear and cytosolic fractions compared with the whole extracts throughout the time course of involution. Results are means $\pm$ S.E.M. ($n = 3$). ANOVA was performed for the statistical analysis where different letters indicate significant differences ($P < 0.05$); 'a' always represents the lowest value within the group.

of mammary acini after 72 h of weaning (Figure 2C, arrowheads), but also in mammary stromal cells (results not shown). Calpains have already been described to localize in the nuclear compartment of adipocytes, being involved in differentiation and adipogenesis in *in vitro* models [27]. During mammary gland involution, programmed cell death of the secretory epithelium takes place concomitant with the repopulation of the mammary fat pad with adipocytes. Indeed, this recolonization of the mammary gland with differentiated adipocytes is observed at 48–72 h after weaning (Supplementary Figure S1A at http://www.biochemj.org/bj/459/bj4590355add.htm). Perilipin, the major lipid droplet-associated protein in adipocytes, was used as a marker to identify adipose tissue. The quantification of the perilipin-stained area showed that adipocyte differentiation was significant from 48 h of weaning onwards (Supplementary Figure S1B). Therefore this time point was chosen for all the experiments related to CAPN1 and adipocyte stromal cells.

To study whether the subpopulation of stromal cells positive for CAPN1 were adipocytes, tissue sections from lactating and 48 h involuting glands were immunostained against CAPN1 and perilipin. As shown in Figure 5(A), CAPN1 was already present in epithelial acini during lactation (left-hand panel); however, the CAPN1 fluorescent signal was significantly higher in the mammary gland after pup removal. In the weaned condition (right-hand panel) CAPN1 was detected both in epithelial tissue and mammary stroma. Indeed, the membrane of these stromal cells positive for CAPN1 was also perilipin-stained, suggesting that CAPN1 was also detectable within adipocytes. It is noteworthy that in these cells, presumably adipocytes, CAPN1 was not merely restricted to the peripheral nuclear membrane, but seemed to internalize within the nuclei (Figure 5A, right-hand panel, arrowheads).

In parallel, *Capn1* mRNA levels increased in adipocyte fractions as weaning progressed (Figure 5B). Activation of this protease was also observed in adipocyte-enriched extracts (Figure 5C, left-hand panel). Although Nup62 cleavage was demonstrated (Figure 5C, right-hand panel) in total tissue, no peripheral NUP degradation was observed in the adipocyte fraction even in 72 h-weaned mammary tissue.

CAPN1 associates with chromatin and histone H3

The results of the present study and previously published data in other models [24,35] suggest that CAPN1 might have different targets in the nuclear compartment of mammary gland cells during involution. Therefore we studied the possible role of CAPN1 in chromatin organization in whole mammary tissue. Fractions of chromatin-enriched and soluble nuclear components were obtained using a nuclear subfractionation method [19] in control or 48 h-weaned glands. To verify appropriate fractionation, both fractions were probed by Western blot analysis for the Nup62,

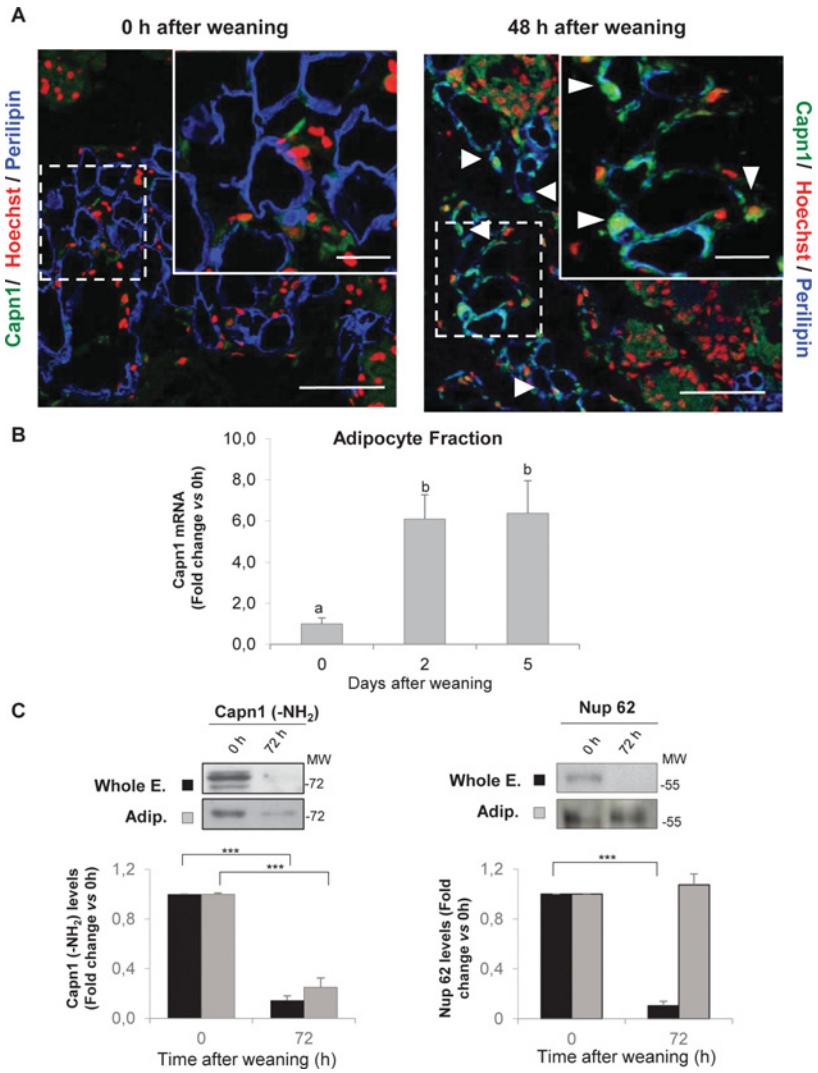

Figure 5 CAPN1 is present in adipocytes during mammary gland involution

(**A**) Representative immunohistochemical analysis of CAPN1 (green), perilipin (blue) and nuclei (Hoechst 33342; red) in tissue sections from mammary glands at the peak of lactation (0 h) and 48 h after litter removal ($n = 3$). Arrowheads show the localization of CAPN1 within the nuclei of perilipin-positive cells at 48 h after weaning and no co-localization within nuclei of adipocytes in control tissue (0 h). Scale bars, 75 μm and 20 μm (magnified section). (**B**) qPCR analysis of *Capn1* mRNA levels in adipocyte fractions isolated from mammary tissue at the peak of lactation (0 h) and after 2 or 5 days of involution. Levels were normalized using *Ipo8* as the housekeeping gene. Results are means $\pm$ S.E.M. ($n = 3$) and ANOVA was performed for the statistical analysis where different superscript letters indicate significant differences ($P < 0.05$); 'a' always represents the lowest value within the group. (**C**) Western blot analysis of CAPN1 N-terminus (left-hand panel) and Nup62 (right-hand panel) in whole mammary gland extracts (black bars) and adipocyte-enriched fraction (grey bars) from control mice (0 h) and mice 72 h after litter removal. Quantification of the bands from 72 h involution compared with control lactating mice levels are shown. Results are means $\pm$ S.E.M. Student's *t* test was performed for the statistical analysis of the protein levels (***$P < 0.001$, 0 h compared with 72 h in whole extracts or adipocyte-enriched fraction).

the NUPs detected by the Mab414 antibody and histone H3 (as a chromatin-enriched-fraction marker). As shown in Figure 6(A) (lower panels), most of NUPs were in the soluble nuclear fraction, whereas histone H3 was mostly in the chromatin-containing fraction. Although the majority of CAPN1 was recovered in the soluble fraction, a significant increase in this protein was also observed in the chromatin-enriched fraction after 48 h of weaning (Figure 6A, upper panels). CAPN2, confined to the nuclear soluble fraction, was increased during weaning when NUPs were degraded. The absence of CAPN2 from the insoluble fraction confirmed the specificity of CAPN1 binding to chromatin.

The co-immunoprecipitated complex CAPN1–H3 detected at 48 h of weaning corroborates the results observed with the nuclear subfractionation (Figure 6B). To further confirm that this interaction was shown in adipocytes, the internalization of CAPN1 within the nucleus was assessed by immunofluorescence staining. Mammary tissue sections from control lactating mice and mice at 48 h after pup removal were stained with antibodies against CAPN1 and histone H3. As shown in Figure 6(C), no co-localization was observed in control lactating mice between CAPN1 (confined mainly to the cytosolic fraction) and histone H3. However, the 48 h-weaned tissue depicts a completely different scenario; the nuclei of adipocytes surrounding the epithelial structures were positive for both CAPN1 and histone H3 (Figure 6C, arrowheads). It is important to highlight that there is also a slight co-localization of these two proteins in the mammary acini during the weaning process. Indeed, in these epithelial cells both a perinuclear and intranuclear subtle yellow staining was observed (Supplementary Figure S2, lower left panel, at http://www.biochemj.org/bj/459/bj4590355add.htm). As we

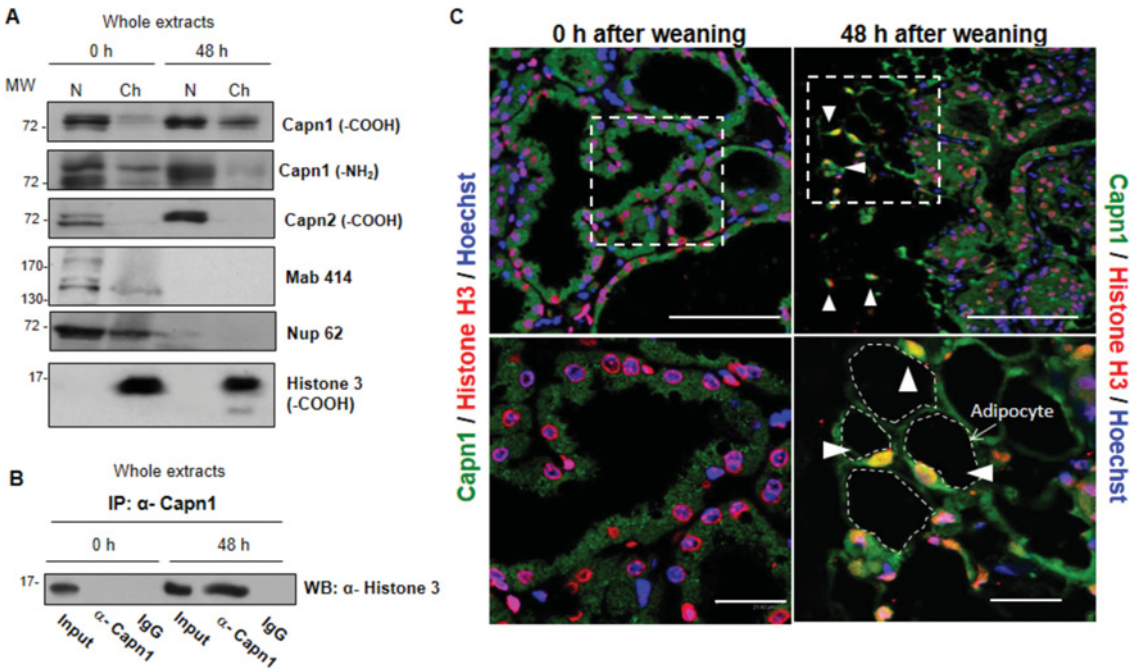

Figure 6 CAPN1 and histone H3 interaction and co-localization in adipocytes

(**A**) Representative Western blot analysis of CAPN1 and CAPN2 in soluble nuclear (N) and chromatin-enriched (Ch) fractions. Anti-Nup62, anti-pan-NUP and anti-(histone H3) (C-terminal domain) were used ($n = 3$). MW, molecular mass. (**B**) Co-immunoprecipitation of CAPN1 and histone H3 in nuclear extracts from control (0 h) and 48 h-involuting glands. Samples were immunoprecipitated (IP) with anti-CAPN1 antibody or unrelated normal serum IgG. The immunoprecipitated CAPN1 was analysed by Western blotting (WB) with an anti-(histone H3) antibody. The image shown is representative of three independent experiments. (**C**) Immunohistochemical analysis of CAPN1 (green), histone H3 (red) and nuclei (Hoechst 33342; blue) co-localization in tissue sections from mammary glands at the peak of lactation (0 h) and 48 h after pup removal ($n = 3$ for each condition). Arrowheads show co-localization of CAPN1 and histone H3 within the nuclei of adipocyte-like cells. The identity of positive cells was confirmed by perilipin staining. Scale bars, 75 μm (upper panels) and 20 μm (lower panels).

have demonstrated previously calpains cleave peripheral NUPs during epithelial cell death, which would explain the thin line of perinuclear dotted staining observed both in all nuclei of mammary epithelial cells and in cells shed in the lumen which have histone H3 labelling (Supplementary Figure S2). On the other hand, calpains have been demonstrated to enter the nucleus upon transient elevation of intracellular calcium, where they can proteolyse transcription factors and nuclear proteins [13,14]. Although we have not identified possible calpain targets within the nuclear compartment of mammary epithelial cells, we cannot rule out this possibility as CAPN1 co-localizes in the nuclei of acini (Figure 6C) and is also observed in chromatin-enriched fractions obtained from total tissue extracts (Figure 6A).

CAPN1 cleaves histone H3 both *in vivo* and *in vitro*

We established that CAPN1 binds to histone H3, but the effect of this interaction is unknown. Activation of other proteases, such as cathepsin L, in the nucleus has already been described, demonstrating that histone H3 is cleaved at its N-terminus during embryonic stem cell differentiation [28]. Thus we wondered whether CAPN1 had a similar effect in our physiological model. Immunoblots of nuclear extracts were probed against different anti-(histone H3) antibodies (including histone H3 C-terminal and N-terminal domain, H3K4me3 and H3K27me3). As shown in Figure 7(A), a faster-migrating band was observed in the samples taken 2 and 3 days after litter removal. Notably, this lower band was only observed when using the anti-(histone H3) C-terminus and anti-H3-K27me3 antibodies. Taken together, these results suggested that an N-terminal fragment of histone H3 was missing during mammary gland involution. To ensure that the cleaved histone H3 observed physiologically was the product of calpain activity, nuclear extracts from calpeptin-treated or *Capn1*-knockdown mice were obtained. Immunoblots against the battery of anti-(histone H3) antibodies were performed on these nuclear extracts after 72 h of weaning, and demonstrated that, upon CAPN1 inhibition (either pharmacologically or by siRNA silencing), the cleaved histone H3 signal was decreased (Figure 7B).

In order to identify the cleaved product an *in vitro* protease reaction was performed. A fragmented histone was observed when recombinant histone H3 and recombinant CAPN1 were incubated (Figure 7C). Furthermore, the band from the cleaved product (Figure 7C, *) was excised from the gel, analysed by MS and identified as histone H3 (12 % coverage and a score of 33.4). On the basis of a molecular mass comparison between bands corresponding to intact and cleaved histone H3, the CAPN1 cleavage site on histone H3 was predicted to be on the N-terminal tail approximately at Lys^{9}–Ser^{10} (Supplementary Figure S3A at http://www.biochemj.org/bj/459/bj4590355add.htm), residues that are highly conserved among species. A calpain cleavage prediction method, based on Multiple Kernel Learning algorithms [29], also predicted the same cleavage site (score 0.14) on histone H3. This prediction would explain why the fragment could not be observed when using antibodies against the cleaved portion of histone H3.

Further *in vitro* experiments were performed to confirm this cleavage. Isolated nuclei from control lactating or 48 h-weaned mammary glands were exposed to recombinant Capn1 or recombinant histone H3. As shown in Figure 7(D), cleaved histone H3 signals appeared in the nuclei of 48 h-weaned glands,

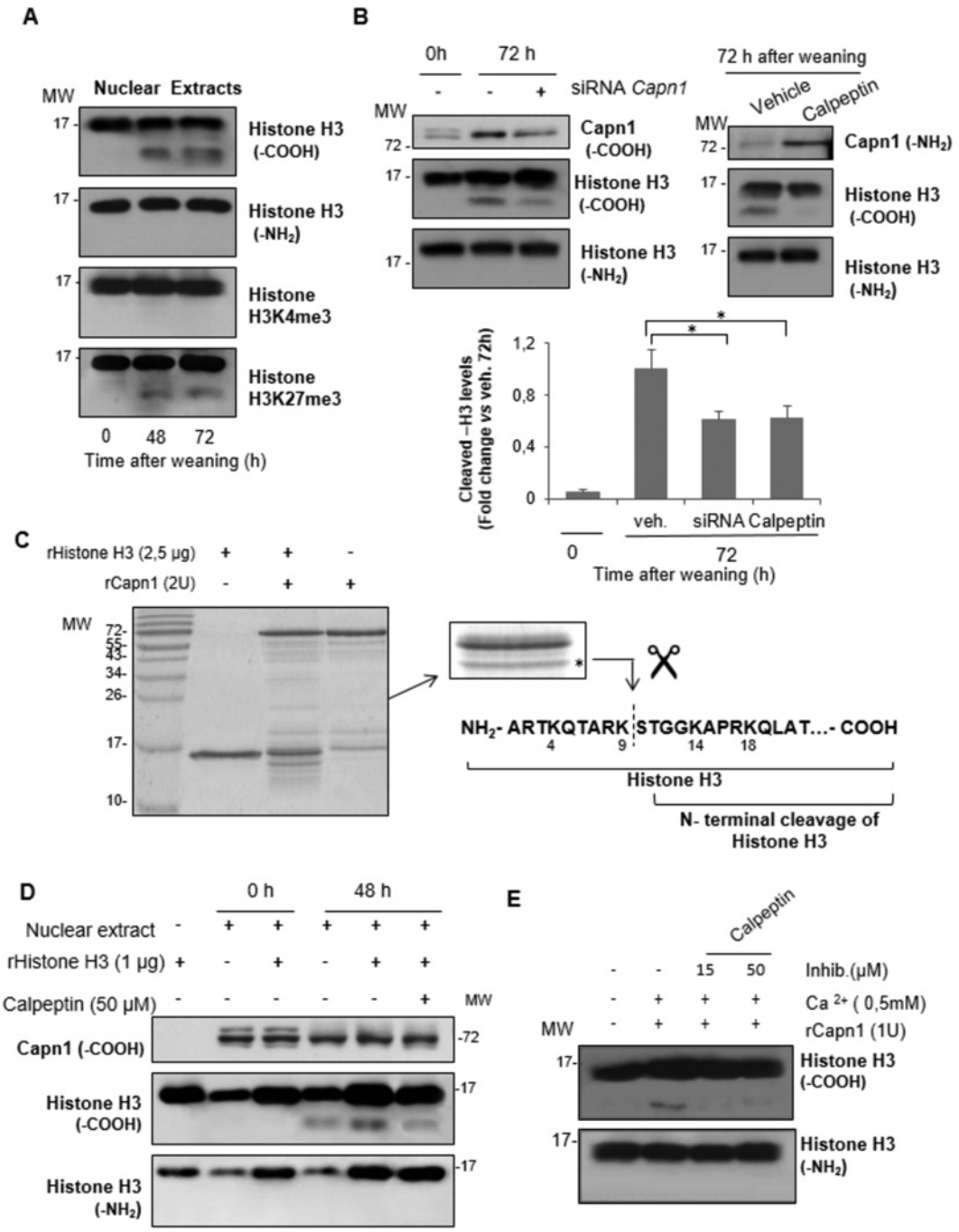

Figure 7 ***In vivo*** **and** ***in vitro*** **cleavage of histone H3 by CAPN1**

(**A**) Representative Western blot analysis of histone H3 in nuclear extracts from control (0 h) and 48 h and 72 h after litter removal. Antibodies recognizing histone H3 (C-terminal domain), histone H3 (N-terminal domain), H3K4me3 or H3K27me3 were used. (**B**) Western blot analysis of histone H3 (antibodies against the N- and C-terminal domain) in extracts from control mice (0 h), 72 h-weaned mice and 72 h-weaned mice where CAPN1 was knocked down (siRNA *Capn1*) (left-hand panel). Western blot analysis of histone H3 in extracts from untreated (vehicle) or calpeptin-treated mammary glands at 72 h of involution (right-hand panel). CAPN1 (C-terminal domain) levels were analysed to confirm the efficiency of the knockdown experiments (left-hand panel) and CAPN1 (N-terminal domain) levels demonstrated CAPN1 inhibition in calpeptin-treated mice (right-hand panel). The histogram shows the quantification of the histone H3-cleaved band. Results are means ± S.E.M. Student's *t* test was performed for the statistical analysis (*$P < 0.05$ compared with vehicle-treated mice). veh., vehicle. In (**A**) and (**B**) three independent mice were used per developmental stage and experimental condition. (**C**) Gel fractionation analysis of recombinant (r) histone H3 incubated in the presence or absence of recombinant Capn1. After Coomassie Blue staining, the band corresponding to the cleaved product (labelled with an asterisk) was excised and analysed by MS. The predicted cleavage site on histone H3 sequence is shown. (**D**) Western blot analysis of histone H3 [antibodies against N- ($-NH_2$) and C-terminal domains (-COOH)] and CAPN1 in nuclear extracts from 0 h and 48 h samples incubated in the presence or absence of recombinant histone H3 and calpeptin ($n = 3$). (**E**) Western blot analysis of histone H3 (antibodies against N- and C-terminal domains) in nuclear extracts from lactating mice (0 h) incubated with recombinant CAPN1 and calcium in the presence of calpeptin ($n = 3$). MW, molecular mass.

where calpains were already activated. Cleaved histone H3 was slightly increased after the addition of recombinant histone H3, but reverted to the 48 h levels when calpeptin was simultaneously added to the nuclear extracts. Similar results were obtained with nuclear extracts from 72 h-weaned samples (Supplementary Figure S3B).

Similarly, the incubation of recombinant CAPN1 with nuclear extracts from control lactating glands produced cleaved histone H3, whereas treatment with calpeptin prevented this cleavage (Figure 7E). Conversely, the same experiment with recombinant CAPN2 did not cleave histone H3 (results not shown). These results provide conclusive evidence that CAPN1 is responsible for histone H3 cleavage during mammary gland involution.

CAPN1 is involved in adipocyte differentiation

Histone H3 was proteolytically processed by CAPN1 in the weaned mammary gland when adipocyte repopulation begins. Undifferentiated cells have been characterized by some epigenetic markers on lineage-specific gene promoters [36]. Nevertheless, transcriptional changes during the differentiation programme do not seem to be limited to specific genes. The global chromatin architecture in undifferentiated cells has a high abundance of euchromatic markers [31,32] compared with differentiated cells [32–35]. We wonder whether the effect of the histone H3 cleavage mediated by CAPN1 could be manifested in a more global way in the weaned mammary gland by the modification of the epigenetic signature. Inmunofluorescence methods have been used previously to correlate the epigenetic distribution and the pluripotent states of cells [36]. This method allows a qualitative study in single cells, an important advantage when working on cell populations that are very heterogeneous such as mammary gland during involution.

In the present study we investigated the global changes in both the distribution of histone modifications and chromatin conformation in the mammary gland when the adipocyte repopulation begins. CAPN1-mediated changes in the epigenetic signature were studied by means of immunohistochemical co-localization of epigenetic marks and CAPN1 in 48 h-weaned mammary tissue sections. Our results show that the euchromatin/active marker H3K4me3, although almost undetectable in epithelial cells, was high in adipocyte-like cells, consistent with an open and dynamic chromatin structure typically found in not fully differentiated cells (Figure 8A, left-hand panel). The low fluorescence intensity of H3K4me3 in the nuclei of epithelial cells was used as the background level, and only signals above this threshold were considered positive. This allowed us to accurately correlate the epigenetic state with the presence of CAPN1 at a single cell level. CAPN1 completely co-localized with H3K4me3 (51 % of the total adipocytes) in a compacted fashion at the nuclear periphery of exclusively non-epithelial mammary cells (Figure 8A, left-hand panel).

On the other hand H3K27me3, a classic marker of repressive chromatin, was found in both epithelial and non-epithelial cells (Figure 8A, right-hand panel). In agreement with this result, the global levels of H3K27me3 have been shown previously to be very similar in pluripotent and differentiated cells [36]. In addition to a significant number of H3K27me3 foci found in both cell types, disperse staining was also observed in the nucleoplasm of non-epithelial cells. A pattern of diffuse heterochromatin markers has been reported to change throughout the differentiated/undifferentiated transition [36]. A double-stained signal for CAPN1 and H3K27me3 was observed in 54 % of the total non-epithelial cells from the mammary stroma. Interestingly, CAPN1 seems to preferentially co-localize with the diffuse nucleoplasmic signal of H3K27me3 found at the nuclear periphery of these non-epithelial cells (73 % of the positive cells showing co-localization had this diffuse pattern).

We reasoned that the CAPN1-mediated cleavage of histone H3 in undifferentiated cells could change the epigenetic signature by removing the active marker on developmentally regulated genes during the differentiation process. Following that rationale, one would expect CAPN1 to have no effect on adipogenic genes whose expression is needed for adipocyte full differentiation. Alternatively, removal of the N-terminal tail of histone H3 could render a more permissive chromatin structure to the adipogenic genes expressed during the differentiation process. Therefore we examined both the effect of the presence of CAPN1 on adipogenic gene promoters by ChIP assay and the expression of these genes in weaned mammary tissue. The *Mbp* gene promoter, a gene not expressed in the mammary gland, was used to assess the specificity of the ChIP experiments. Interestingly, we found that CAPN1 was associated with the *Cebpa* and *Lep* promoters after 48 h of weaning (Figure 8B). These two adipogenic genes are involved in terminal differentiation and the acquisition of the adipocyte phenotype respectively. As expected, the expression of both genes was induced during the differentiation process when compared with the peak of lactation (Figure 8C). These results do not discard our hypothesis, but indicate a more complex mechanism behind the effect of CAPN1. Indeed, although the role of CAPN1-mediated cleavage of histone H3 in chromatin organization remains unknown, we cannot rule out the possibility that CAPN1 is involved in the transition or reorganization of heterochromatin towards the cell differentiation program.

DISCUSSION

The mammary gland undergoes extensive changes during the pregnancy/lactation cycle. Among the different pathways that control mammary gland involution, the calpain system has been already recognized as a key mediator of programmed cell death not only in mammary gland [9], but also in other experimental models [37,38]. At the end of lactation, upon calcium increase [39] calpains become activated and translocate to both the mitochondria and lysosomal organelles [1,9]. The present study focuses on the role of CAPN1 on nuclear targets both in epithelial and non-epithelial cells during involution.

Activation of calpains results in the cleavage of several proteins, mainly located in the plasma membrane, but also in other organelles [37,40,41]. First, the results of the present study show that CAPN1 translocates to the nuclear membrane as weaning progresses, where it cleaves different cytoplasmic NUPs (Figure 2A). Furthermore, although CAPN1 and CAPN2 are able to cleave NUPs *in vitro* (Figure 6C) our experiments blocking CAPN1 (by either calpeptin administration or siRNA against *Capn1*) showed that only CAPN1 can specifically cleave different NUPs *in vivo*. Owing to their essential role in controlling nucleocytoplasmic transport, the cytosolic degradation of several NUPs by calpains would potentially induce a loss of nuclear membrane integrity in the epithelial cells of acini. These structural changes of the nuclear envelope and NPC ultimately would trigger the redistribution of pro-apoptotic factors and the subsequent amplification of the death signal. In agreement with this, recent findings have demonstrated that during calcium-mediated neuronal degeneration, NPC components can be degraded increasing channel permeability that leads to final disassembly of the nuclear envelope and neuronal cell death [25]. We observed a spread distribution of CAPN1 in the mammary acini during weaning that was not restricted to the dead epithelial cells shed into the lumen of alveoli (Supplementary Figure S2). Therefore our finding that nuclear ‘leakiness’ is dramatically accelerated during mammary gland involution suggests that the accumulation of damage at the NPC structure might be a crucial event in the loss of nuclear integrity that precedes cell death.

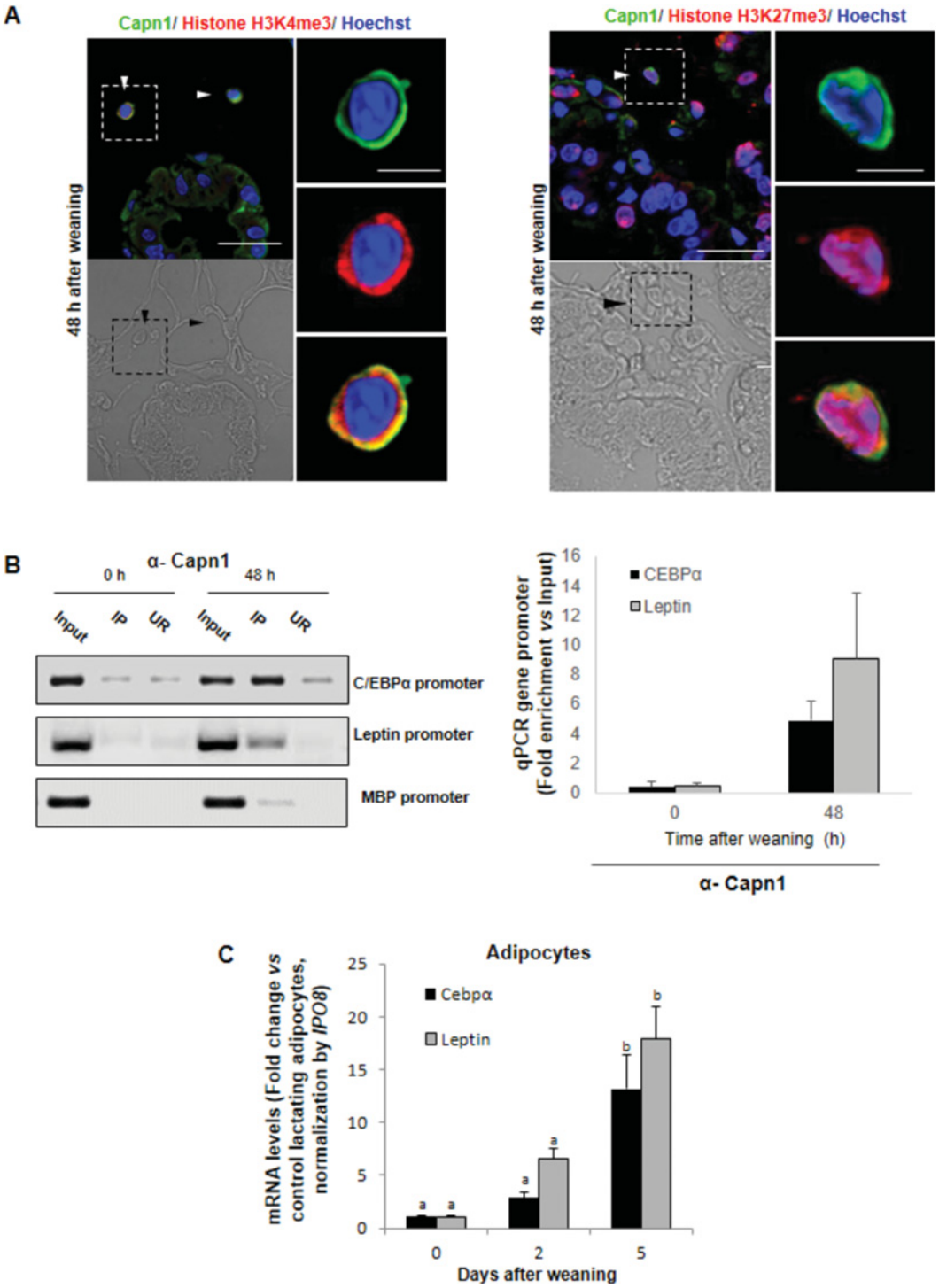

Figure 8 CAPN1 distribution and binding to gene promoters during adipocyte terminal differentiation

(**A**) Representative immunofluorescence analysis of CAPN1 (green), H3K4me3 (red; left-hand panel), H3K27me3 (red; right-hand panel) and nuclei (Hoechst 33342; blue) distribution in tissue sections from mammary glands at 48 h after litter removal. Arrowheads show the co-localization of CAPN1 with specific epigenetics markers on histone H3 within the nuclei of adipocytes. Scale bars, 40 μm or 10 μm (magnified sections). (**B**) CAPN1 binding to *Cebpa*, *Lep* or *Mbp* gene promoters was analysed by ChIP assay in mammary gland homogenates from control (0 h) and 48 h-weaning mice. A representative analysis of three independent experiments is shown (left-hand panel). qPCR data of *Capn1* bound to *Cebpa* (black bars) or *Lep* (grey bars) gene promoters is represented as the fold enrichment compared with the input. Results are means ± S.E.M. (**C**) Gene expression analysis of *Cebpa* and *Lep* genes by qPCR in adipocyte-enriched fractions at different times after weaning ($n = 3$). Levels were normalized using *Ipo8* as a housekeeping gene. Results are means ± S.E.M. ANOVA was performed for the statistical analysis and different letters indicate significant differences ($P < 0.05$); 'a' always represents the lowest value within the group.

Secondly, the results of the present study also show a role for CAPN1 on non-membrane proteins. We present evidence for the presence of CAPN1 in the nuclei of adipocytes, as can be concluded by the fact that the stromal cells showing nuclear CAPN1 localization are also positive for perilipin, an adipocyte marker (Figure 5A). Although the preferential distribution of

CAPN1 seemed to be different in adipocytes (nuclear) compared with epithelial cells (cytosolic), we cannot rule out the possibility of CAPN1 also having a role in the nuclear compartment of epithelial cells during weaning. Nevertheless, our results strongly suggest a dual function for CAPN1 in both cell types during involution: (i) although in epithelial cells CAPN1 cleaves NUPs, in the adipocyte-enriched fractions the NUPs remained intact (Figure 5C); (ii) CAPN1 and histone H3 co-localization seems to be restricted to adipocytes (Figures 5, 6 and 8 and Supplementary Figure S2); (iii) in control lactating samples, where most of cells are epithelial cells, CAPN1 and CAPN2 are detected only in the nuclear soluble fraction (Figure 6A). This fraction is most probably enriched in nuclear membrane proteins and their associated proteins in agreement with a role for CAPN1 in the permeabilization of the NPC, but not in histone H3 cleavage. Conversely, CAPN1 is present in the chromatin-enriched fraction after 48 h of weaning; a time point characterized by massive epithelial cell death and fat pad repopulation with adipocytes.

Most importantly, we show for the first time in the present study that histone H3 is a new target of CAPN1. Moreover, although histone H3 cleavage mediated by other cysteine proteases has been described in cultured cells [28] to our knowledge this is the first indication of an *in vivo* endogenous cleavage of H3 in mammals. Our *in vivo* and *in vitro* experiments revealed that CAPN1 cleaves the N-terminal tail of histone H3. This was reinforced by the *in vitro* experiments showing that CAPN1 can cleave histone H3 in a direct fashion. Regarding the specificity of CAPN1-mediated histone H3 cleavage compared with CAPN2 or cathepsins, we can conclude that the latter cysteine proteases are not involved in this process for several reasons: CAPN2, as mentioned above, is not present in the chromatin-enriched fraction (Figure 6); we found no effect of recombinant CAPN2 on histone H3 from the 48 h-weaning samples (results not shown); *Capn1* knockdown increased the intact/cleaved-H3 ratio at 72 h weaning (Figure 7); calpeptin, blocked H3 cleavage. Nevertheless, we cannot exclude a role for other cysteine proteases throughout the time course of mammary gland involution.

CAPN1 is a regulator of adipocyte differentiation in *in vitro* models and embryonic development [27]. Although the functional consequences of CAPN1-mediated cleavage of histone H3 remain elusive, it is tempting to speculate that removal of epigenetic marks might serve to change the epigenetic signature of selected genes upon adipocyte differentiation. The same hypothesis was already managed to explain the effect of cathepsin L on histone H3 proteolysis in cultured embryonic stem cells [28]. Alternatively, H3 proteolysis could be understood as a potential mode of transcriptional regulation by the creation of new histone H3 N-terminal tails to establish a new epigenetic program. Removal of repressive epigenetic marks on differentiation genes, or prevention of new activating marks on pluripotency genes, would render the precise pattern of gene expression during adipocyte differentiation.

In addition, the epigenetic markers on histone H3 could recruit CAPN1 to selected genes leading to cleaved histone H3. It has been published previously that the promoters of genes playing key functions in development and differentiation processes present the bivalent signal of H3K4me3 and H3K27me3 [30]. The nuclear localization of these 'bivalent' genes was found along the nuclear border in immature cells and dramatically rearranged towards the central nucleoplasm in differentiated cells [42,43]. On the basis of results of the present study and these previous works, CAPN1 localized at the nuclear periphery could proteolyse histone H3 at the promoters of adipogenic genes with this bivalent signal. The effect of this cleavage could be the acquisition of a laxer chromatin structure on these specific genes. However, we cannot exclude an alternative or additional role for CAPN1 on transcription factors bound to gene promoters. Indeed, CAPN1 is involved in the activation of several transcription factors [17,27]. Intriguingly, CAPN1 does not contain a DNA-recognition motif and, therefore, it should be recruited by other proteins to gene promoters. A question that remains to be resolved is the identity of such proteins. CAPN1 and transcription factors could follow the same model as described for cofactors with enzymatic activity such as HATs (histone acetyltransferases) and HDACs (histone deacetylases). Once recruited to gene promoters by transcription factors, these enzymes will modify both the transcription factor-binding activity and the acetylation of proximal histone H3 N-terminal tails. An alternative possibility is that post-translational modifications at the N-terminal tails of histone H3 could act as docking sites for CAPN1 binding to specific gene loci.

In the present study the major role that calpains play in the involuting mammary gland after the pregnancy/lactation cycle has been emphasized. Compelling evidence shows that these proteases play a role in overlapping processes during involution. On the one hand, the targets of calpains within the lysosomal, mitochondrial and nuclear membranes induce membrane leakiness and favour cell death. Meanwhile, Capn1 is most probably involved in the modulation of pre-adipocyte differentiation to mature adipocytes through chromatin remodelling and activation of specific adipogenic genes and/or repression of developmental genes.

AUTHOR CONTRIBUTION

Teresa Arnandis and Ivan Ferrer-Vicens performed the experiments. Concha García was in charge of mice and obtained the tissue samples. Luis Torres, Elena Garcia-Trevijano, Rosa Zaragoza and Juan Viña contributed to the study design and data interpretation. Rosa Zaragoza, Elena Garcia-Trevijano and Juan Viña drafted the initial report, and all authors contributed to the final draft of the paper.

ACKNOWLEDGEMENTS

We thank Sonia Priego for acquiring the confocal microscopy images and Jaime Ferrer and Elisa Alonso-Yuste for tissue histology.

FUNDING

This work was supported by the Spanish Government PN I+D+I 2008-2011 [grant number BFU2010-18253 (to J.R.V.)], the ISCIII including FEDER [grant number PI12/02394 (to E.R.G.-T.)], the Consellería de Educación [grant number GVPROMETEO 2010-075 (to I.F.-V.)] and the Fundación INCLIVA (to R.Z.). T.A. is the recipient of a pre-doctoral fellowship from the Ministerio de Educación.

REFERENCES

1 Kreuzaler, P. A., Staniszewska, A. D., Li, W., Omidvar, N., Kedjouar, B., Turkson, J., Poli, V., Flavell, R. A., Clarkson, R. W. E. and Watson, C. J. (2011) Stat3 controls lysosomal-mediated cell death *in vivo*. Nat. Cell Biol. **13**, 303–309
2 Clarkson, R. W. E., Wayland, M. T., Lee, J., Freeman, T. and Watson, C. J. (2004) Gene expression profiling of mammary gland development reveals putative roles for death receptors and immune mediators in post-lactational regression. Breast Cancer Res. **6**, 92–109
3 Stein, T., Morris, J. S., Davies, C. R., Weber-Hall, S. J., Duffy, M. A., Heath, V. J., Bell, A. K., Ferrier, R. K., Sandilands, G. P. and Gusterson, B. A. (2004) Involution of the mouse mammary gland is associated with an immune cascade and an acute-phase response, involving LBP, CD14 and STAT3. Breast Cancer Res. **6**, 75–91
4 Zaragozá, R., Miralles, V. J., Rus, A. D., García, C., Carmena, R., García-Trevijano, E. R., Barber, T., Pallardó, F. V., Torres, L. and Viña, J. R. (2005) Weaning induces NOS-2 expression through NF-κB modulation in the lactating mammary gland: importance of GSH. Biochem. J. **391**, 581–588
5 Haricharan, S. and Li, Y. (2013) STAT signaling in mammary gland differentiation, cell survival and tumorigenesis. Mol. Cell. Endocrinol. **382**, 560–569

6 Zaragozá, R., Bosch, A., García, C., Sandoval, J., Serna, E., Torres, L., García-Trevijano, E. R. and Viña, J. R. (2010) Nitric oxide triggers mammary gland involution after weaning: remodelling is delayed but not impaired in mice lacking inducible nitric oxide synthase. Biochem. J. **428**, 451–462
7 Zaragozá, R., Gimeno, A., Miralles, V. J., García-Trevijano, E. R., Carmena, R., García, C., Mata, M., Puertes, I. R., Torres, L. and Viña, J. R. (2007) Retinoids induce MMP-9 expression through RARα during mammary gland remodeling. Am. J. Physiol. Endocrinol. Metab. **292**, 1140–1148
8 Torres, L., Serna, E., Bosch, A., Zaragozá, R., García, C., Miralles, V. J., Sandoval, J., Viña, J. R. and García-Trevijano, E. R. (2011) NF-κB as node for signal amplification during weaning. Cell. Physiol. Biochem. **28**, 833–846
9 Arnandis, T., Ferrer-Vicens, I., García-Trevijano, E. R., Miralles, V. J., García, C., Torres, L., Viña, J. R. and Zaragozá, R. (2012) Calpains mediate epithelial-cell death during mammary gland involution: mitochondria and lysosomal destabilization. Cell Death Differ. **19**, 1536–1548
10 Campbell, R. L. and Davies, P. L. (2012) Structure–function relationships in calpains. Biochem. J. **447**, 335–351
11 Goll, D. E., Thompson, V. F., Li, H., Wei, W. and Cong, J. (2003) The calpain system. Physiol. Rev. **83**, 731–801
12 Suzuki, K., Hata, S., Kawabata, Y. and Sorimachi, H. (2004) Structure, activation, and biology of calpain. Diabetes **53**, 12–18
13 Neuberger, T., Chakrabarti, A. K., Russell, T., DeVries, G. H., Hogan, E. L. and Banik, N. L. (1997) Immunolocalization of cytoplasmic and myelin mcalpain in transfected Schwann cells: I. Effect of treatment with growth factors. J. Neurosci. Res. **47**, 521–530
14 Watt, F. and Molloy, P. L. (1993) Specific cleavage of transcription factors by the thiol protease, m-calpain. Nucleic Acids Res. **21**, 5092–5100
15 Ball, J. R. and Ullman, K. S. (2005) Versatility at the nuclear pore complex: lessons learned from the nucleoporin Nup153. Chromosoma **114**, 319–330
16 Yajima, Y. and Kawashima, S. (2002) Calpain function in the differentiation of mesenchymal stem cells. Biol. Chem. **383**, 757–764
17 Patel, Y. M. and Lane, M. D. (1999) Role of calpain in adipocyte differentiation. Proc. Natl. Acad. Sci. U.S.A. **96**, 1279–1284
18 Musri, M. M., Gomis, R. and Párrizas, M. (2010) A chromatin perspective of adipogenesis. Organogenesis **6**, 15–23
19 Wysocka, J., Reilly, P. T. and Herr, W. (2001) Loss of HCF-1-chromatin association precedes temperature-induced growth arrest of tsBN67 cells. Mol. Cell. Biol. **21**, 3820–3829
20 Rodbell, M. (1964) Metabolism of isolated fat cells. I. Effects of hormones on glucose metabolism and lipolysis. J. Biol. Chem. **239**, 375–380
21 Mandal, P., Azad, G. K. and Tomar, R. S. (2012) Identification of a novel histone H3 specific protease activity in nuclei of chicken liver. Biochem. Biophys. Res. Commun. **421**, 261–267
22 Hurtado del Pozo, C., Calvo, R. M., Vesperinas-García, G., Gómez-Ambrosi, J., Frühbeck, G., Corripio-Sánchez, R., Rubio, M. A. and Obregon, M. J. (2010) *IPO8* and *FBXL10*: new reference genes for gene expression studies in human adipose tissue. Obesity **18**, 897–903
23 Chakrabarti, A. K., Neuberger, T., Russell, T., Banik, N. L. and DeVries, G. H. (1997) Immunolocalization of cytoplasmic and myelin mcalpain in transfected Schwann cells: I. Effect of withdrawl of growth factors. J. Neurosci. Res. **47**, 609–616
24 Chou, S. M., Huang, T. H., Chen, H. C. and Li, T. K. (2011) Calcium-induced cleavage of DNA topoisomerase I involves the cytoplasmic-nuclear shuttling of calpain 2. Cell. Mol. Life Sci. **68**, 2769–2784
25 Bano, D., Hengartner, M. O. and Nicotera, P. (2010) Nuclear pore complex during neuronal degeneration. Nucleus **1**, 136–138
26 D'Angelo, M. A., Raices, M., Panowski, S. H. and Hetzer, M. W. (2009) Age-dependent deterioration of nuclear pore complexes causes a loss of nuclear integrity in post-mitotic cells. Cell **136**, 284–295
27 Yajima, Y., Sato, M., Sorimachi, H., Inomata, M., Maki, M. and Kawashima, S. (2006) Calpain system regulates differentiation of adult primitive mesenchymal ST-13 adipocytes. Endocrinology **147**, 4811–4819
28 Duncan, E. M., Muratore-Schroeder, T. L., Cook, R. G., Garcia, B. A., Shabanowitz, J., Hunt, D. F. and Allis, C. D. (2008) Cathepsin L proteolytically processes histone H3 during mouse embryonic stem cell differentiation. Cell **135**, 284–294
29 DuVerle, D. A., Ono, Y., Sorimachi, H. and Mamitsuka, H. (2011) Calpain cleavage prediction using multiple kernel learning. PLoS One **6**, e19035
30 Verrier, L., Vandromme, M. and Trouche, D. (2011) Histone demethylases in chromatin cross-talks. Biol. Cell **103**, 381–401
31 Meshorer, E., Yellajoshula, D., George, E., Scambler, P. J., Brown, D. T. and Misteli, T. (2006) Hyperdynamic plasticity of chromatin proteins in pluripotent embryonic stem cells. Dev. Cell **10**, 105–116
32 Efroni, S., Duttagupta, R., Cheng, J., Dehghani, H., Hoeppner, D. J., Dash, C., Bazett-Jones, D. P., Le Grice, S., McKay, R. D., Buetow, K. H. et al. (2008) Global transcription in pluripotent embryonic stem cells. Cell Stem Cell **2**, 437–447
33 Ahmed, K., Dehghani, H., Rugg-Gunn, P., Fussner, E., Rossant, J. and Bazett-Jones, D. P. (2010) Global chromatin architecture reflects pluripotency and lineage commitment in the early mouse embryo. PLoS One **5**, e10531
34 Fussner, E., Djuric, U., Strauss, M., Hotta, A., Perez-Iratxeta, C., Lanner, F., Dilworth, F. J., Ellis, J. and Bazett-Jones, D. P. (2011) Constitutive heterochromatin reorganization during somatic cell reprogramming. EMBO J. **30**, 1778–1789
35 Gaspar-Maia, A., Alajem, A., Meshorer, E. and Ramalho-Santos, M. (2011) Open chromatin in pluripotency and reprogramming. Nat. Rev. Mol. Cell Biol. **12**, 36–47
36 Mattout, A., Biran, A. and Meshorer, E. (2011) Global epigenetic changes during somatic cell reprogramming to iPS cells. J. Mol. Cell Biol. **3**, 341–350
37 Liu, L., Xing, D. and Chen, W. R. (2009) Micro-calpain regulates caspase-dependent and apoptosis inducing factor-mediated caspase-independent apoptotic pathways in cisplatin-induced apoptosis. Int. J. Cancer **125**, 2757–2766
38 Nozaki, K., Das, A., Ray, S. K. and Banik, N. L. (2011) Calpeptin attenuated apoptosis and intracellular inflammatory changes in muscle cells. J. Neurosci. Res. **89**, 536–543
39 Reinhardt, T. A. and Lippolis, J. D. (2009) Mammary gland involution is associated with rapid down regulation of major mammary Ca^{2+}-ATPases. Biochem. Biophys. Res. Commun. **378**, 99–102
40 Kar, P., Samanta, K., Shaikh, S., Chowdhury, A., Chakraborti, T. and Chakraborti, S. (2010) Mitochondrial calpain system: an overview. Arch. Biochem. Biophys. **495**, 1–7
41 Tremper-Wells, B. and Vallano, M. L. (2005) Nuclear calpain regulates Ca^{2+}-dependent signaling via proteolysis of nuclear Ca^{2+}/calmodulin-dependent protein kinase type IV in cultured neurons. J. Biol. Chem. **280**, 2165–2175
42 Musri, M. M., Corominola, H., Casamitjana, R., Gomis, R. and Párrizas, M. (2006) Histone H3 lysine 4 dimethylation signals the transcriptional competence of the adiponectin promoter in preadipocytes. J. Biol. Chem. **281**, 17180–17188
43 Szczerbal, I., Foster, H. A. and Bridger, J. M. (2009) The spatial repositioning of adipogenesis genes is correlated with their expression status in a porcine mesenchymal stem cell adipogenesis model system. Chromosoma **118**, 647–663

Received 26 June 2013/22 January 2014; accepted 27 January 2014
Published as BJ Immediate Publication 27 January 2014, doi:10.1042/BJ20130847

Biochem. J. (2014) **459**, 355–368 (Printed in Great Britain) doi:10.1042/BJ20130847

online data

SUPPLEMENTARY ONLINE DATA

Differential functions of calpain 1 during epithelial cell death and adipocyte differentiation in mammary gland involution

Teresa ARNANDIS*, Ivan FERRER-VICENS*, Luis TORRES*, Concha GARCÍA*, Elena R. GARCIA-TREVIJANO*, Rosa ZARAGOZA* and Juan R. VIÑA*[1]

*Departamento de Bioquímica y Biología Molecular, Fundación Investigación Hospital Clínico-INCLIVA, Facultad de Medicina, Universidad de Valencia, Valencia 46010, Spain

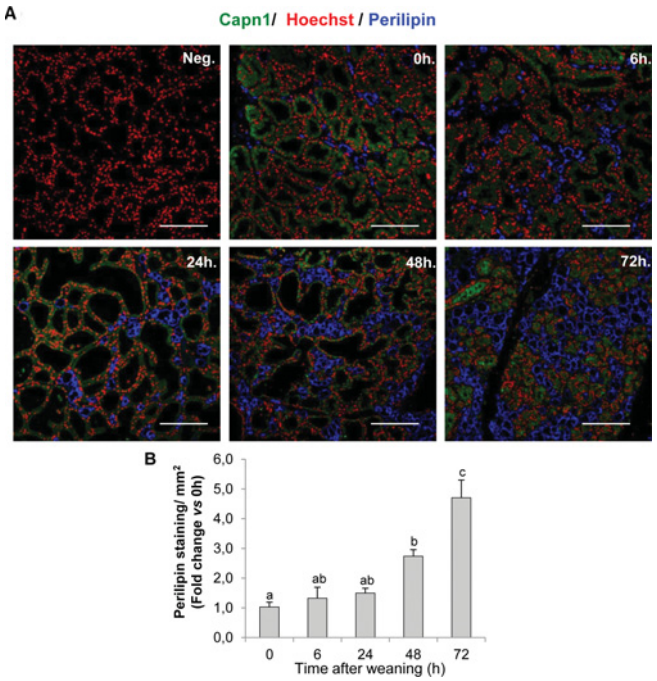

Figure S1 Time course of adipocyte repopulation during mammary gland involution

(**A**) Mammary tissue sections were immunostained with CAPN1 (green), perilipin (blue) as an adipocyte marker and Hoechst 33342 (red) as a nuclear marker in control lactating (0 h) and involuting mammary glands (6, 24, 48 and 72 h after pup removal). Autofluorescence and non-specific binding was reduced using samples incubated with secondary antibody (Neg.). Scale bars, 150 μm. (**B**) Adipocyte repopulation during the time course of involution is represented as the fold change compared with the control (0 h). Adipocyte fold change was determined by quantification of perilipin signal/mm^2 shown in (**A**). Three separate mice were used per developmental stage. Results are means$\pm$S.E.M. ANOVA was performed for the statistical analysis and different letters indicate significant differences ($P < 0.05$); 'a' always represents the lowest value within the group.

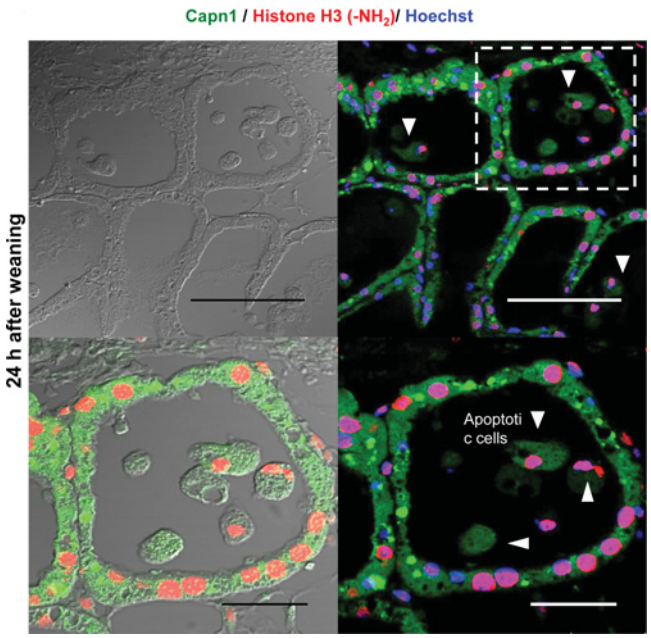

Figure S2 Co-localization of CAPN1 and histone H3 in mammary gland acini

Representative immunofluorescence analysis for CAPN1 (green) and histone H3 (red) in mammary gland alveoli 24 h after pup removal. Arrowheads show apoptotic cells shed into the alveolar lumen. Note the highly condensed nuclei. Scale bars, 75 μm (upper panels) and 20 μm (lower panels).

[1] To whom correspondence should be addressed (email Juan.R.Vina@uv.es).

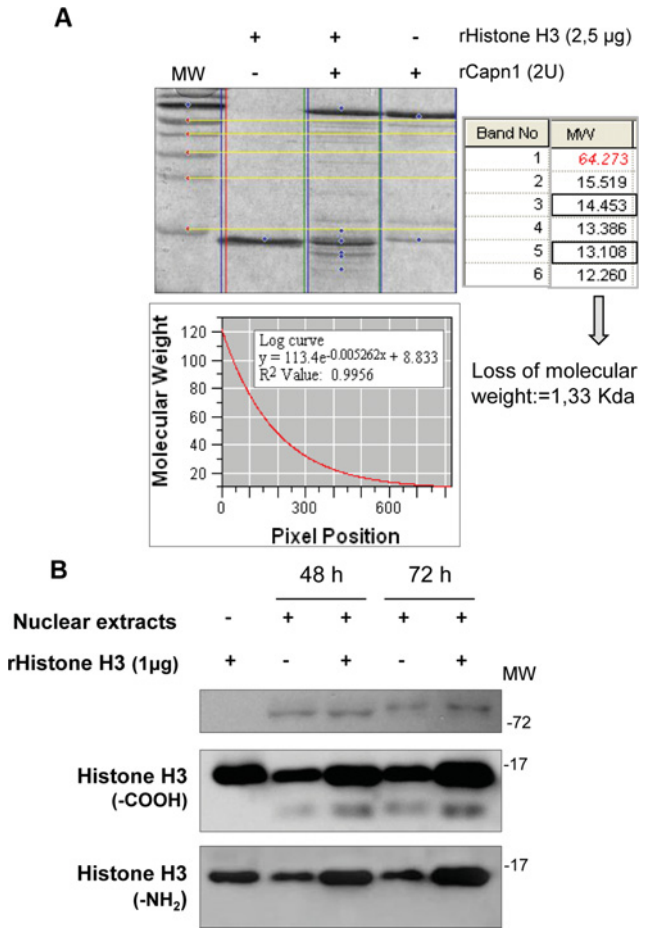

Figure S3 ***In vitro*** **proteolysis of recombinat histone H3 by CAPN1**

(**A**) A molecular mass analysis of the histone H3 truncated band. The protein ladder fits with a logarithmic curve from which the molecular mass of the bands were extrapolated. The difference in molecular mass from the two main bands represents the loss of the N-terminal tail of the histone. (**B**) Mammary gland nuclear extracts were incubated in the presence or absence of recombinant (r) histone H3. Levels of CAPN1 and the N- and C-terminal domains of histone H3 were assessed by Western blotting at 48 and 72 h after litter removal. A representative image of three different experiments is shown. MW, molecular mass.

Received 26 June 2013/22 January 2014; accepted 27 January 2014
Published as BJ Immediate Publication 27 January 2014, doi:10.1042/BJ20130847